DOI: 10.1002/cmdc.201402085

Diazepinoporphyrazines Containing Peripheral Styryl Substituents and Their Promising Nanomolar Photodynamic Activity against Oral Cancer Cells in Liposomal Formulations

Jaroslaw Piskorz,*[a] Krystyna Konopka,[b] Nejat Düzgüneş,[b] Zofia Gdaniec,[c] Jadwiga Mielcarek,[a] and Tomasz Goslinski*[d]

The photochemical properties and photodynamic activity of three porphyrazines (Pzs) containing annulated diazepine rings, including novel demetalated porphyrazine-possessing bis(styryl)diazepine moieties were investigated. The porphyrazines were evaluated in terms of their electronic absorption and emission properties, their tendency to undergo aggregation and photodegradation, as well as their singlet oxygen generation efficiency. The in vitro photodynamic activity of the porphyrazines and their liposomal formulations were examined by using two oral squamous cell carcinoma cell lines. Magnesium(II) tribenzodiazepinoporphyrazine (**1**) revealed the highest phototoxic effect in both cell lines used, H413 and HSC-3. Encapsulation of Pz**1** into L-α-phosphatidyl-D,L-glycerol:1-palmitoyl-2-oleoyl-*sn*-glycero-3-phosphocholine liposomes resulted in a nearly threefold increase in photocytotoxicity relative to that of the solution of Pz**1** (IC_{50} values of 45 and 129 nM, respectively).

Introduction

Photodynamic therapy (PDT) is a medical treatment that uses light to activate a drug called a photosensitizer in the presence of oxygen, and this leads to local damage by the generation of reactive oxygen species. PDT is used to cure various cancers and noncancer diseases including age-related macular degeneration, oral leukoplakia, and oral lichen planus. Moreover, PDT can be applied to the treatment of bacterial, fungal, parasitic, and viral infections.[1–4]

Many porphyrinoid macrocycles, including porphyrins, phthalocyanines, chlorins, and porphyrazines (Pzs), have been investigated as photosensitizers for PDT.[5–10] Pzs possessing peripherally annulated diazepine rings have been elaborated on by the Ercolani and Stuzhin groups.[11–14] They stipulated that the physicochemical properties of these macrocycles result from the conjugation of the diazepine ring with the macrocyclic core. The UV/Vis spectra of tetrakis-2,3-(5,7-diphenyl-1,4-diazepino)porphyrazine and its various metal complexes revealed a broad and split Q-band with maximum absorption wavelengths in the 630–640 and 660–680 nm ranges. The presence of an additional band at 660–680 nm is the result of an n–π* transition between the lone pairs of electrons of the nitrogen atoms in the diazepine rings and the π electrons of the macrocyclic core.[11] In addition, tribenzoporphyrazine containing an annulated 5,7-diphenyl-6*H*-1,4-diazepine ring and its magnesium(II) complex exhibited significantly red-shifted Q-bands up to 715 and 700 nm, respectively.[15] The red-shifted Q-band absorptions observed for diazepinoporphyrazines suggest that these macrocycles might be considered as potential photosensitizers for photodynamic therapy, as light of longer wavelength is able to penetrate deeper into the irradiated tissue.[16] We recently reported the synthesis of novel porphyrazines bearing styryldiazepine and bis(styryl)diazepine substituents with UV/Vis absorption maxima shifted up to 729 and 704 nm, respectively.[17,18]

Although the synthesis of new PDT candidates is of increasing interest, special efforts are made to design various forms of nanocarriers for photosensitizers, of which liposomes are considered one of the best and most promising. The application of liposomes as porphyrinoid delivery systems can overcome many of the drawbacks of conventional photosensitizers, such as high lipophilicity, lack of solubility in aqueous media, tendency to undergo aggregation, poor tissue penetration, and

[a] *J. Piskorz, Prof. J. Mielcarek*
Department of Inorganic & Analytical Chemistry
Poznan University of Medical Sciences
Grunwaldzka 6, 60-780 Poznan (Poland)
E-mail: piskorzj@ump.edu.pl

[b] *Prof. K. Konopka, Prof. N. Düzgüneş*
Department of Biomedical Sciences, University of the Pacific
Arthur A. Dugoni School of Dentistry
2155 Webster Street, San Francisco, CA 94115 (USA)

[c] *Prof. Z. Gdaniec*
Institute of Bioorganic Chemistry
Polish Academy of Sciences, Z. Noskowskiego 12, Poznan (Poland)

[d] *Dr. T. Goslinski*
Department of Chemical Technology of Drugs
Poznan University of Medical Sciences
Grunwaldzka 6, 60-780 Poznan (Poland)
E-mail: tomasz.goslinski@ump.edu.pl

Supporting information for this article is available on the WWW under http://dx.doi.org/10.1002/cmdc.201402085.

low bioavailability. Moreover, liposomes can facilitate the development of novel effective photosensitizers.[19–22]

In this paper, we report the photochemical properties and photodynamic activity of three Pzs containing annulated diazepine rings, including a novel demetalated one possessing a bis(styryl)diazepine moiety. We evaluated their electronic absorption and emission properties, their tendency to undergo aggregation and photodegradation, as well as their efficiency in generating singlet oxygen. The in vitro photodynamic activity of Pzs and their liposomal formulations was examined by using two human oral squamous cell carcinoma cell lines.

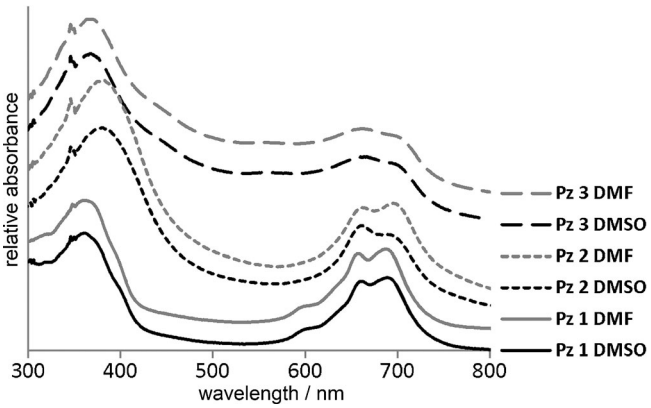

Figure 1. UV/Vis spectra for Pzs **1**–**3**.

Results and Discussion

Synthesis and characterization

Magnesium(II) diazepinotribenzoporphyrazine (**1**) and magnesium(II) diazepinoporphyrazine (**2**) were synthesized according to previously described procedures.[17,18] Demetalated diazepinoporphyrazine (**3**) was synthesized from the magnesium complex by treatment with trifluoroacetic acid by using published procedures,[23,24] and it was characterized by using UV/Vis spectroscopy, MALDI MS, and various NMR spectroscopy techniques, including ^{1}H–^{1}H COSY, ^{1}H–^{13}C HSQC, and ^{1}H–^{13}C HMBC (Scheme 1; see also Figure S1 and Table S1, Supporting Information).

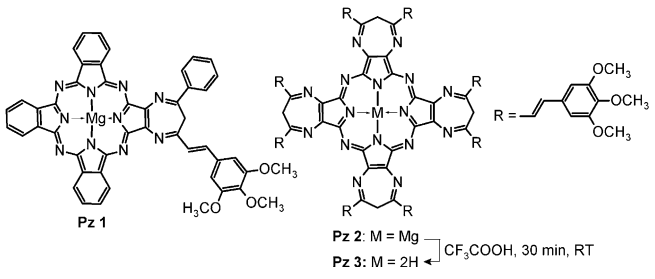

Scheme 1. Structures of Pzs **1**–**3**.

Electronic absorption and emission properties

The absorption spectra of Pz**1** recorded in DMF and DMSO revealed a Soret band with maximum absorption at 358 and 364 nm, respectively. In addition, a broad Q-band, split into two sub-bands at 658/689 and 658/692 nm, respectively, was observed. Pz**2** exhibited UV/Vis spectra that were similar to those of Pz**1**, but the absorption maxima were bathochromically shifted to 378, 661, and 689 nm in DMF and to 381, 661, and 695 nm in DMSO. Demetalated analogue Pz**3** revealed less intense absorption bands with a Soret band at 368 nm and a broad, flat Q-band at 662 and 664 nm in DMF and DMSO, respectively (Figure 1 and Table S2).

The UV/Vis spectra of Pzs **1**–**3** dissolved at different concentrations in DMF or DMSO were used for aggregation behavior studies. The correlations between the absorbance of the Q-band maximum and the concentrations of the macrocyclic compounds were evaluated. Although these correlations were linear for all compounds, statistical analysis revealed that the Beer–Lambert law was obeyed only for Pz**1** (Figure S2 and Table S3). These data indicate that Pz**2** and Pz**3**, unlike Pz**1**, aggregate in both DMF and DMSO. Aggregate formation is a common problem in photodynamic therapy, because self-association of the photosensitizer molecules decreases the generation of singlet oxygen, which thus hinders the photosensitizing efficiency.[25]

The fluorescence emission spectra of Pz**1** in DMF or DMSO showed maxima at 707 and 708 nm, respectively. The fluorescence quantum yield (Φ_F) values of 2.6×10^{-2} in DMF and 4.5×10^{-2} in DMSO were calculated by following the method given by Chauke et al.[26] Less intense fluorescence with a maximum at 716 nm and with $\Phi_F=4.1\times10^{-3}$ was found for Pz**2** in DMF and with $\Phi_F=1.8\times10^{-3}$ in DMSO. The weakest fluorescence emission bands were observed for Pz**3** at 671 ($\Phi_F=3.1\times10^{-5}$) and 675 nm ($\Phi_F=5.5\times10^{-5}$) in DMF and DMSO, respectively (Figure 2).

Photodegradation

The susceptibility of Pzs **1**–**3** to degradation upon exposure to light was determined by observing the changes in the UV/Vis spectra during irradiation in both DMF and DMSO. The absorption bands decreased upon irradiation, and there was no formation of new bands. Thus, it seems that light absorption leads to degradation of the macrocycles into smaller fragments that are not able to absorb light in the visible region.[27] Photodegradation was much faster in DMF than in DMSO, and it followed first-order kinetics for all the macrocycles studied (Table 1; detailed kinetic parameters are shown in Table S4); the first-order plots are presented in Figure 3.

The photodegradation measured in DMF for metalated Pz**1** and Pz**2** took place in two stages and for demetalated Pz**3** in one stage. This observation is consistent with that obtained for a series of porphyrazines with 2,5-dimethylpyrrol-1-yl and dimethylamino substituents.[28] For all three compounds, the photochemical decomposition in DMSO took place in two stages. Moreover, it was found that ~30% of Pz**1** and Pz**2** and

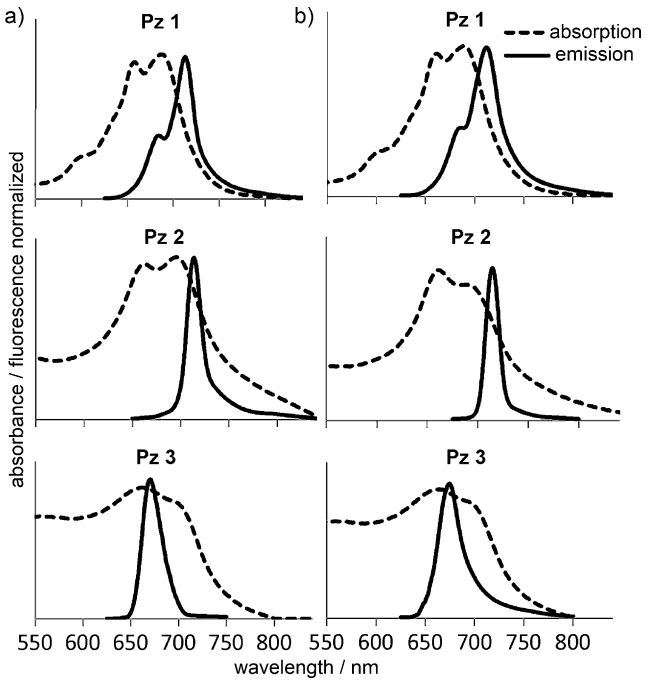

Figure 2. The Q-band absorption and emission spectra of Pzs **1**–**3** in a) DMF and b) DMSO.

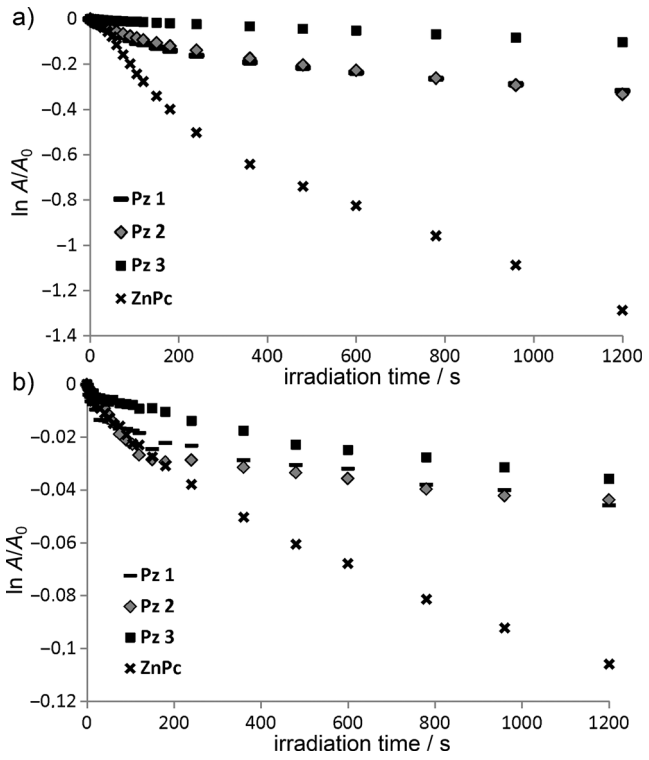

Figure 3. Photodegradation first-order plots of Pzs **1**–**3** in a) DMF and b) DMSO.

Table 1. Photodegradation kinetic parameters of Pzs **1**–**3**.

Compd	DMF			DMSO		
	Stage	$t_{0.5}$ [s]	Pz degraded [%]	Stage	$t_{0.5}$ [s]	Pz degraded [%]
Pz**1**	I	73.4	27.3 ± 0.3	I	19.3	4.5 ± 0.3
	II	4700		II	30400	
Pz**2**	I	87.5	28.3 ± 0.4	I	62.8	4.3 ± 0.2
	II	3900		II	36500	
Pz**3**	I	8140	9.4 ± 0.4	I	195	3.5 ± 0.1
				II	37400	
ZnPc	I	69.4	72.4 ± 3.2	I	122	10.1 ± 0.5
	II	914		II	10500	

~10% of Pz**3** was degraded in DMF after 20 min of irradiation. Similarly, in DMSO, demetalated analogue Pz**3** was the most stable (3.5% degradation upon exposure to light for 20 min). However, all the porphyrazines studied were found to be much more stable during irradiation than zinc(II) phthalocyanine (ZnPc).

Singlet oxygen generation

The potential photodynamic activities of Pzs **1**–**3** were evaluated by measuring their ability to generate singlet oxygen. The relative method, with ZnPc as a reference and 1,3-diphenylisobenzofuran (DPBF) as a chemical quencher for singlet oxygen, was applied.[29,30] Solutions containing Pzs **1**–**3** or ZnPc in a mixture with DPBF in DMF or DMSO were irradiated with monochromatic light at wavelengths corresponding to their Q-band maxima. The kinetics of DPBF decomposition by photogenerated singlet oxygen was studied by monitoring the absorbance decrease at 417 nm, and they were used to calculate the singlet oxygen generation yields (Φ_Δ). The results obtained are given in Table 2 (detailed kinetic parameters are shown in Table S5). The first-order plots are presented in Figure 4.

Table 2. Quantum yields for the generation of singlet oxygen by using Pzs **1**–**3**.

Compd	$\Phi_\Delta \pm \Delta\Phi_\Delta$[a]	
	DMF	DMSO
Pz **1**	0.281 ± 0.006	0.311 ± 0.003
Pz **2**	0.109 ± 0.006	0.013 ± 0.001
Pz **3**	0.0039 ± 0.0003	0.0054 ± 0.0005
ZnPc	0.56[31]	0.67[31]

[a] Results are given with 95% confidence.

Pz**1** was found to be the most efficient singlet oxygen generator, with high Φ_Δ values of 0.28 and 0.31 in DMF and DMSO, respectively, although these values are lower than those of ZnPc ($\Phi_{\Delta DMF} = 0.56$; $\Phi_{\Delta DMSO} = 0.67$).[31] Pz**2** showed a moderate ability to form singlet oxygen in DMF, but a weak ability in DMSO, whereas the lowest Φ_Δ values in both solvents were obtained for demetalated Pz**3** (Table 2). The decreased generation of singlet oxygen by Pz**2** in DMSO seems to result from its aggregation.[18] The considerably lower Φ_Δ values for demetalated Pz**3** relative to those of its metal complex Pz**2** match with the results obtained for other Pzs and their metal complexes.[28,32,33]

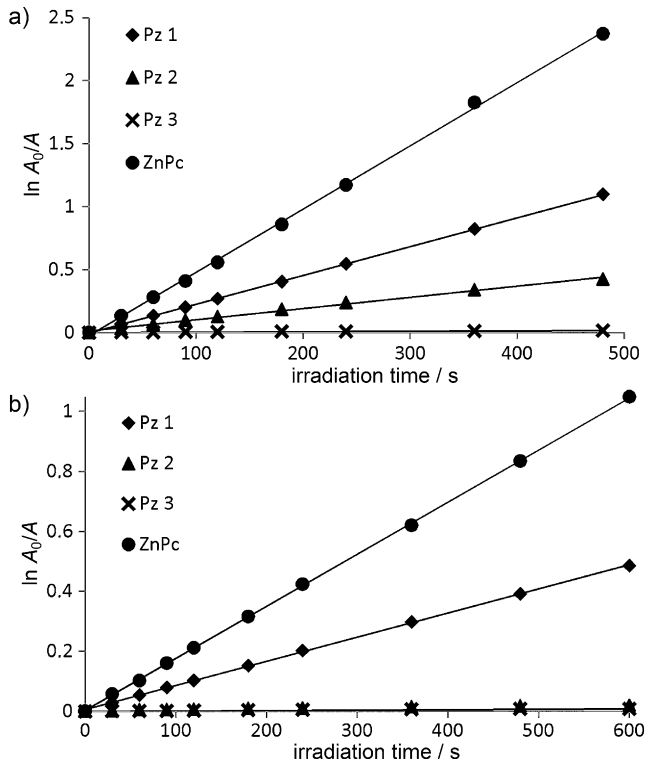

Figure 4. First-order plots of DPBF degradation (in air) by singlet oxygen photogenerated during irradiation of Pzs **1**–**3** in a) DMF and b) DMSO.

In vitro photodynamic activity

The photodynamic activity of Pzs **1**–**3** was investigated in vitro by using two oral squamous cell carcinoma cell lines, HSC-3 derived from the tongue and H413 derived from the buccal mucosa. Dark toxicities of Pzs **1**–**3** were evaluated in the limited concentration range from 0.1 to 10 μM, because of the massive aggregation of Pz**2** and Pz**3** at higher concentrations. The viability of both cell lines was unaffected by Pz**2** and Pz**3** at all the concentrations used, whereas Pz**1** was toxic only to H413 cells at concentrations higher than 1 μM (Table S6). Noteworthy, the dark toxicity results correspond well to those obtained previously for other photosensitizers, for which a higher sensitivity of H413 to HSC-3 cells was observed.[34]

The light-induced toxicities were examined only at the concentrations that had not caused any dark toxicity. HSC-3 and H413 cells were incubated with Pz**1** at 0.05, 0.25, 1 μM and with Pz**2** and Pz**3** at 0.1, 1, and 10 μM for 24 h. Next, they were irradiated for 20 min with light of 690 nm from a high-power light-emitting diode multichip emitter (Roithner Lasertechnik, 9.8 V). The light intensity at the surface of the plate was set to 3.0 mW cm^{-2} and the total light dose was 3.6 J cm^{-2}. Cell viability was quantified by the Alamar Blue assay. It was found that Pz**1** at 1 μM decreased the viability of H413 cells by 90% and that Pz**2** at 10 μM decreased the viability by ~25%, whereas Pz**3** did not show any significant light-induced cytotoxicity (Table S7). In addition, Pz**1** also exhibited the highest phototoxic effect in HSC-3 cells, with a decrease in cell viability by ~95% at 1 μM. Pz**2** did not show any phototoxic effect, whereas Pz**3** decreased the viability of HSC-3 cells by 87% at 10 μM (Figure 5 and Table S8).

The insolubility of Pzs **1**–**3** in water and their strong tendency to form aggregates encouraged us to incorporate them into liposomes, which are known to be promising delivery systems for photosensitizers that can overcome these limitations.[21] Pz**1** and Pz**3** showed a high phototoxic effect against HSC-3 cells and were encapsulated into liposomes.

Their photodynamic efficacy was researched in four different liposome formulations that were prepared by a thin-film hydration method: 1) L-α-phosphatidyl-D,L-glycerol (PG, from chicken eggs:1-palmitoyl-2-oleoyl-*sn*-glycero-3-phosphocholine (POPC), 2) PG:POPC:cholesterol (Chol), 3) *N*-[1-(2,3-dioleoyloxy)-propyl]-*N*,*N*,*N*-trimethylammonium chloride (DOTAP):POPC, and 4) DOTAP:POPC:Chol.[34,35] The mean diameter of the extruded liposomes containing Pz**1** and Pz**3** varied from 123.4 to 167.5 nm and from 199.8 to 330.3 nm, respectively (Table S9). Light-induced cytotoxicity against HSC-3 cells of liposomes with incorporated Pz**1** were examined at concentrations of 0.05, 0.25, and 1 μM and with incorporated Pz**3** at concentrations of 0.1, 1.0, 10 μM. All four types of liposomes containing Pz**1** revealed a high photocytotoxic effect. However, liposomes with incorporated Pz**3** were not cytotoxic (Table S10). Further experiments were performed at six concentrations with Pz**1**

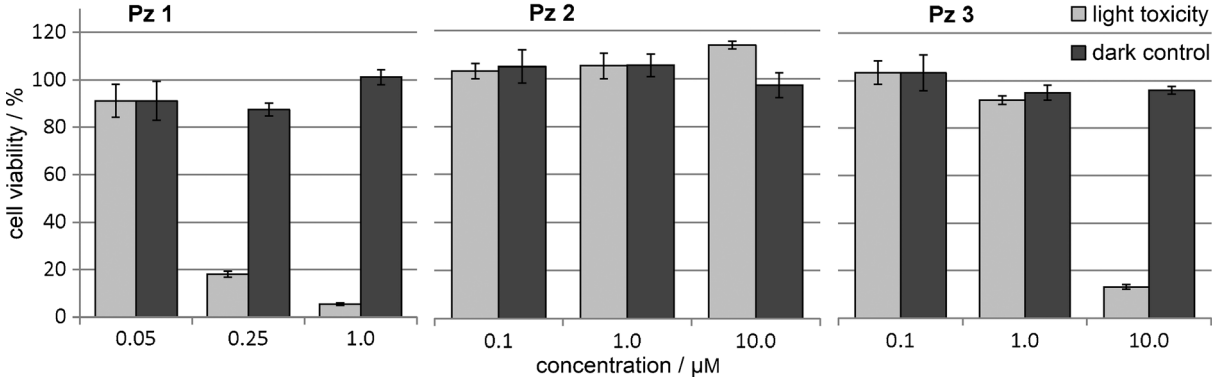

Figure 5. Light toxicity (and dark control) of Pzs **1**–**3** against HSC-3 cells. Data represent the mean ± standard deviation for experiments performed in triplicate.

(IC_{50} = 129 nM) and its four liposomal formulations (IC_{50} = 45–150 nM) and with Pz**3** (IC_{50} = 4590 nM). Negatively charged liposomes containing Pz**1** (Pz**1**:PG:POPC and Pz**1**:PG:POPC:Chol) showed higher cytotoxicity than the free compound and positively charged Pz**1** liposomes (Pz**1**:DOTAP:POPC, Figure 6). Noteworthy, the IC_{50} value for the most active Pz**1**:PG:POPC

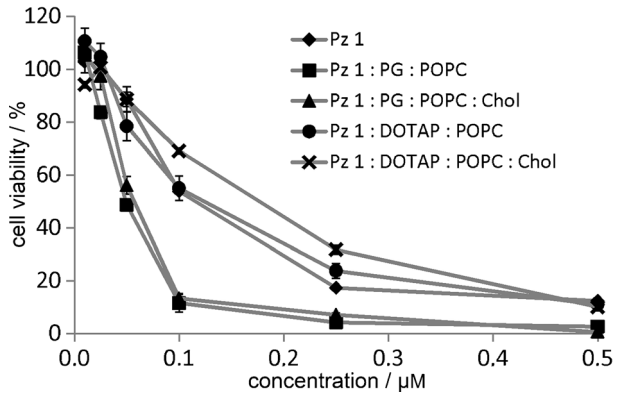

Figure 6. Phototoxic effect of Pz**1** and its liposomal formulations on HSC-3 cells. Data represent the mean ± standard deviation for experiments performed in triplicate.

liposomes was almost three times lower than that determined for free-form Pz**1** in solution, which indicates that these liposomes are the most potent delivery systems for photosensitizer Pz**1** (Table 3).

Table 3. Cytotoxicity of liposome-encapsulated photosensitizers against HSC-3 cells as a means to determine the photodynamic efficacy of the liposomal formulations.

Liposomal formulation[a]	IC_{50} [nM]
Pz**1**	129
Pz**1**:PG:POPC	45
Pz**1**:PG:POPC:Chol	52
Pz**1**:DOTAP:POPC	126
Pz**1**:DOTAP:POPC:Chol	150
Pz**3**	4590

[a] PG = L-α-phosphatidyl-D,L-glycerol, POPC = 1-palmitoyl-2-oleoyl-*sn*-glycero-3-phosphocholine, Chol = cholesterol, DOTAP = *N*-[1-(2,3-dioleoyloxy)propyl]-*N*,*N*,*N*-trimethylammonium chloride (DOTAP).

The subcellular localization of Pz**1** and Pz**3** was investigated by fluorescence microscopy by incubating HSC-3 cells with the photosensitizers and the organelle-specific fluorescent dyes MitoTracker Green FM (mitochondria), Alexa Fluor 350 WGA (plasma membrane), Syto 13 (nucleic acids), and Hoechst 33342 (nucleus).[8,36] It was found that the fluorescence from the mitochondria overlaps with the fluorescence from both the macrocycles, which confirms that they accumulate inside the cells. In addition, images showing fluorescence from both compounds could not be merged with images of other dyes, which suggests that Pz**3** is mainly localized in the mitochondrial area, whereas Pz**1** is partially localized in this area (Figure S3). It was reported that porphyrinoid photosensitizers localizing in mitochondria are the most effective.[37,38]

Conclusions

Three Pzs containing annulated diazepine rings, including novel demetalated porphyrazine possessing the bis-(styryl)diazepine moiety, were investigated in terms of their photochemical properties and their photodynamic activity. Magnesium(II) tribenzoporphyrazine (**1**) showed the highest fluorescence quantum yield and the highest singlet oxygen generation quantum yield but the lowest tendency to undergo aggregation. In addition, Pz**1** revealed the highest phototoxic effect in both oral squamous cell carcinoma lines used, H413 and HSC-3. Moreover, encapsulation of Pz**1** into L-α-phosphatidyl-D,L-glycerol:1-palmitoyl-2-oleoyl-*sn*-glycero-3-phosphocholine liposomes resulted in photocytotoxicity that was almost three times higher than that of the free form of Pz**1** in solution, with IC_{50} values of 45 and 129 nM, respectively. These results indicate that Pz**1** encapsulated in liposomes might be considered as a promising antitumor agent for further preclinical photodynamic therapy studies.

Experimental Section

Chemistry

General: All reactions were conducted in oven-dried glassware under an atmosphere of argon. All solvents and reagents were obtained from commercial suppliers and used without further purification. Flash column chromatography was performed on Merck silica gel 60, particle size 40–63 μm, and Fluka silica gel 90 C_{18} reverse phase. Thin-layer chromatography (TLC) was performed on silica gel Merck Kieselgel 60 F_{254} and DC Kieselgel 60 RP-18 F_{254}s plates and visualized with UV light (λ_{max} = 254 or 365 nm). NMR spectra were recorded with a Bruker Avance II spectrometer operating at a frequency of 400 MHz for ^{1}H and 100 MHz for ^{13}C. Chemical shifts (δ) are quoted in parts per million (ppm) and are referenced to a residual solvent peak. Coupling constants (*J*) are quoted in Hertz (Hz). The abbreviations, s, d, and h, refer to singlet, doublet, and hidden signal, respectively. Additional techniques (^{1}H–^{1}H COSY, ^{1}H–^{13}C HSQC, ^{1}H–^{13}C HMBC) were used to assist with allocation assignment. Mass spectra (MALDI TOF) were performed by the Advanced Chemical Equipment and Instrumentation Facility at the Faculty of Chemistry, Adam Mickiewicz University, Poznan. The purity of all compounds was determined by HPLC analysis performed with an Agilent 1200 Series and was found to be ≥95%.

Tetrakis[5,7-bis{(*E*)-2-(3,4,5-trimethoxyphenyl)ethenyl}-6*H*-1,4-diazepino][2,3-*b*;2′,3′-*g*;2″,3‴-*l*;2⁗,3⁗′-*q*]porphyrazine (3): Magnesium(II) porphyrazine (**2**; 232 mg, 0.1 mmol) was dissolved in trifluoroacetic acid (15 mL) in the dark, and the mixture was stirred for 30 min at room temperature. The solution was then poured into iced water (300 mL) and neutralized with saturated $NaHCO_3$. The organic phase was extracted with CH_2Cl_2. The solvent was removed under reduced pressure, and the crude residue was purified by chromatography (normal phase, dichloromethane/methanol = 50:1 to 20:1 *v*/*v*; reverse phase, methanol/tetrahydrofuran = 25:1 *v*/*v*) to give **3** (33 mg, 14%). R_f = 0.35 (dichloromethane/methanol = 20:1 *v*/*v*). ^{1}H NMR (400 MHz, [D_5]pyridine): δ = 8.52 (d, ^3J = 16 Hz,

8H; 8 C5(7)-CH=CH), 8.17 (d, ^3J=16 Hz, 8H; 8 C5(7)-CH=CH), 7.04 (s, 16H; 16 ArH), 6.75 (d, ^2J=12 Hz, 4H; 4 N=C-CH$_2$), 5.86 (d, ^2J=12 Hz, 4H; 4 N=C-CH$_2$), 3.99 (s, 24H; 8 OCH$_3$), 3.85 (s, 48H; 16 OCH$_3$), −3.63 ppm (s, 2H; 2 NH). ^{13}C NMR (100 MHz, [D$_5$]pyridine): δ=154.2, 154.0, 150.2, 142.9, 140.7, 140.4, 132.0, 128.6, 105.8, 60.5, 56.0, 38.8 ppm (unresolved, observed in ^{1}H–^{13}C HSQC and ^{1}H–^{13}C HMBC, see the Supporting Information). UV/Vis (DMF): λ_{max} (log ε)=368 (4.14), 662 nm (4.58). UV/Vis (DMSO): λ_{max} (log ε)=368 (4.14), 664 nm (4.56). MS (MALDI): *m/z* (%): 2117 $[M+H]^+$ (calcd for $[M+H]^+$ 2116.83).

Photochemical studies

The UV/Vis spectra were recorded in the range from 200 to 900 nm by using a Shimadzu UV-160A spectrophotometer with PC 160 PLUS manual. Fluorescence spectra were recorded by using a Jasco 6200 spectrofluorimeter. The fluorescence quantum yields were calculated by using Equation (1):

$$\Phi_F = \Phi_{Freference}\left(\frac{F_{sample}}{F_{reference}}\right)\left(\frac{A_{reference}}{A_{sample}}\right) \quad (1)$$

in which *F* and *A* correspond to the measured area under the emission band and the absorbance at the excitation position (360 nm), respectively.[26] ZnPc was used as a reference ($\Phi_{F\ ZnPc}$=0.17 in DMF; $\Phi_{F\ ZnPc}$=0.20 in DMSO).[39,40] A 150 W high-pressure xenon lamp (Optel) was used as a light source for photodegradation studies. Solutions of Pzs **1**–**3** and ZnPc in DMF or DMSO with absorbance set at ~0.7 were irradiated in a 1 cm path-length cylindrical cell (2.8 mL) with the light over 450 nm owing to the use of a yellow glass cut-off filter (HCC16). The light intensity was set to 130 klux (luxmeter TES-1335).[28,41]

The quantum yields of the singlet oxygen generation were determined in DMSO and DMF solutions (3.0 mL, no oxygen bubbled) by using the relative method with zinc(II) phthalocyanine (ZnPc, Sigma–Aldrich) as a reference and 1,3-diphenylisobenzofuran (DPBF) as a chemical quencher for singlet oxygen, following recently presented methodologies.[29,30] Solutions of Pzs **1**–**3** or ZnPc in DMF and DMSO in the presence of DPBF were irradiated in a 1 cm path-length quartz cell (3 mL) with monochromatic light by using a 150 W high-pressure Xe lamp (Optel) through a monochromator M250/1200/U. The irradiation wavelengths were adjusted to the maximum of the absorption bands at the Q-bands characteristic of each compound (absorbance of the sensitizers ≈0.5). The concentration of DPBF was set to ~3×10^{-5} mol L^{-1} to avoid chain reactions induced by DPBF in the presence of singlet oxygen.[42] The light intensity was set to 0.5 mW cm^{-2} (Radiometer RD 0.2/2 with TD probe, Optel). All experiments were performed in air (without bubbling oxygen or air though the solvent) at ambient temperature. The samples were kept in the dark before irradiation.

Biological methods

Cell culture: HSC-3 cells, derived from squamous cell carcinoma (SCC) of the tongue,[43] were provided by Dr. R. Kramer (University of California, San Francisco, UCSF, USA). H413 cells, derived from SCC of the buccal mucosa,[44] were obtained from Dr. R. Jordan (UCSF). HSC-3 cells were cultured in Dulbecco's modified Eagle medium (DMEM), supplemented with 10% (*v/v*) heat-inactivated fetal bovine serum (FBS), penicillin (100 U mL^{-1}), streptomycin (100 μg mL^{-1}), and L-glutamine (4 mM) (DMEM/10). H413 cells were maintained in DMEM/10 supplemented with Ham's Nutrient Mixture F12 (DMEM/10/F12). Cells were incubated in tissue culture flasks at 37 °C in a humidified atmosphere containing 5% CO_2 and were then passaged 1:6 twice a week by using a trypsin-ethylenediaminetetraacetic acid (EDTA) solution. All media, penicillin–streptomycin solution, L-glutamine, FBS, trypsin-EDTA, phosphate-buffered saline (PBS), and Dulbecco's phosphate buffered saline (DPBS), were obtained from the UCSF Cell Culture Facility, San Francisco, USA. Photosensitizers were dissolved in dimethyl sulfoxide (Sigma–Aldrich) and subsequently diluted in DMEM or DMEM/F12 (without FBS and phenol red) to obtain the desirable concentration of the photosensitizer used in the experiments. The DMSO concentration in the final solution did not exceed 0.5%.

Dark toxicity: One day before the experiment, HSC-3 and H413 cells were seeded in 48-well plates at a density of 1.8×10^5 and 1.4×10^5 cells per well, respectively, in medium (1 mL, with FBS and phenol red) and used at ~80% confluence. Subsequently, cells were prewashed twice with PBS (0.5 mL), and the medium (1 mL, without FBS and phenol red) containing the photosensitizer at a given concentration was added to each well except for those containing the controls. FBS-free media were used to avoid binding of photosensitizers to the serum proteins. After the 24 h incubation at 37 °C, cells were washed twice with PBS, complete medium (1 mL) was added to each well, and the cells were incubated for 24 h at 37 °C. Cell viability was quantified by the Alamar Blue assay (see below). Cells incubated either with medium alone or medium/0.5% DMSO served as controls.

Light-dependent toxicity: One day before the experiment, HSC-3 and H413 cells were seeded in 48-well plates at a density of 1.8×10^5 and 1.4×10^5 cells per well, respectively, in complete medium (1 mL) and used at ~80% confluence. Cells were prewashed twice with PBS, and the medium (1 mL, without FBS and phenol red) containing the photosensitizer was added to each well except for those containing the controls. The cells were incubated for 24 h at 37 °C, washed twice with PBS, and the medium (without FBS and phenol red) was added. Subsequently, the cells were irradiated for 20 min with light of wavelength 690 nm from a high-power light-emitting diode multichip emitter (Roithner Lasertechnik, 9.8V). The light intensity at the surface of the plate was set to 3.0 mW cm^{-2} measured by a Thorlabs TM100A optical power meter, and the total light dose was 3.6 J cm^{-2}. One plate from each experiment was not exposed to light, and it served as a control. Directly after light exposure, medium (without FBS and phenol red) was replaced with complete medium (1 mL), and the cells were incubated for 24 h at 37 °C. Cell viability was quantified by the Alamar Blue assay (see below).

Cell viability: Cell morphology was evaluated by Nikon TMS inverted-phase contrast microscopy at 100× magnification. The number of viable cells used for the experiments was determined by the Trypan Blue exclusion assay (Gibco-Invitrogen Corporation). Cell viability was quantified by a modified Alamar Blue assay.[45,46] Briefly, 10% (*v/v*) Alamar Blue dye (1.0 mL) in the appropriate complete medium was added to each well. After incubation at 37 °C for 2–3 h, the supernatant (200 μL) was assayed by measuring the absorbance at 570 and 600 nm. Cell viability (as a percentage of control cells) was calculated according to Equation (2):

$$\text{Cell viability} = \frac{[(A_{570}-A_{600})\text{ of test cells}]}{[(A_{570}-A_{600})\text{ of control cells}]}\times 100\,\% \quad (2)$$

Liposome preparation: 1-Palmitoyl-2-oleoyl-*sn*-glycero-3-phosphocholine (POPC), L-α-phosphatidyl-D,L-glycerol (chicken egg, PG), *N*-[1-(2,3-dioleoyloxy)propyl]-*N*,*N*,*N*-trimethylammonium chloride

(DOTAP), and cholesterol (Chol) were purchased from Avanti Polar Lipids, Inc. (Alabaster, AL, USA). Four different liposome formulations were prepared by a thin-film hydration method.[34,35] Appropriate amounts of the lipid solutions in chloroform (POPC, 20 mg mL^{-1}; PG, 25 mg mL^{-1}; DOTAP, 10 mg mL^{-1}; Chol, 10 mg mL^{-1}) and photosensitizer (0.4 mg mL^{-1}) were placed in glass tubes, mixed, and evaporated to dryness by using a rotary evaporator. Films formed on the bottom of glass tubes were dried overnight in a vacuum oven at room temperature to evaporate any remaining chloroform. Subsequently, the dried films were hydrated with HEPES buffered saline {10 mM HEPES [*N*-(2-hydroxyethyl)piperazine-*N*′-(2-ethanesulfonic acid)], 140 mM NaCl, pH 7.5} and dispersed by vortexing for 5–10 min. The resulting liposome suspensions were passed 21 times through polycarbonate membranes with a pore diameter of 100 nm by using a syringe extruder (Avanti Polar Lipids) to obtain unilamellar liposomes with a uniform size distribution. The molar ratios of ingredients in final liposome formulations were: 1) Pzs **1**–**3** (0.1), PG (2), POPC (8); 2) Pz**1** or Pz**3** (0.1), PG (1.33), POPC (5.34) Chol (3.33); 3) Pz**1** or Pz**3** (0.1), DOTAP (2), POPC (8); and 4) Pz**1** or Pz**3** (0.1), DOTAP (1.33), POPC (5.34) Chol (3.33). The liposome size was determined by dynamic light scattering measurements by using a Coulter N4 Plus particle size analyzer (Beckman). Samples were stored at 2–8 °C under an atmosphere of argon and were protected from light. The final concentration of the photosensitizer achieved in the liposome suspensions was 100 μM. These suspensions were diluted with DME medium without FBS to achieve appropriate concentration for biological activity evaluation on HSC-3 cells. Free liposomes without photosensitizers were prepared as controls.

Subcellular localization studies: HSC-3 cells were seeded in 48-well plates at a density of 1.8×10^5 and incubated for 24 h at 37 °C. Subsequently, cells were washed and medium (1 mL, without FBS and phenol red) containing the photosensitizer and Pz**1** at 1 μM or Pz**3** at 10 μM was added. After the 24 h incubation at 37 °C, cells were washed twice with PBS, and the solutions of the dyes in PBS were added and incubated for MitoTracker Green FM (Molecular Probes, 0.4 μM) 15 min, Alexa Fluor 350 WGA (Molecular Probes, 5 μg mL^{-1}) 15 min, Syto 13 (Molecular Probes 5 μM) 30 min, and Hoechst 33342 (Molecular Probes, 6 μM) 30 min. Next, the cells were washed with PBS. Fluorescence micrographs were obtained with a Nikon Diaphot inverted fluorescence microscope equipped with filters, (Chroma Technology Corporation, Bellows Falls, USA) 49006 filter for Pzs **1** and **3**, 61000v2 filter for MitoTracker and Syto 13, 49000 filter for Alexa Fluor 350 and Hoechst 33342, and a Jenaoptik digital camera by using the ProgRes Capture Software. The cells were observed by using a 20× phase contrast objective.

Statistical analysis

Data were compared for statistical significance by the unpaired Student's t-test by using StatView software (Brain Power Inc., Calabasas, CA). A probability value (*P*) of less than 0.05 was considered significantly different.

Acknowledgements

The authors thank Beata Kwiatkowska, Senait Gebremedhin, and Michael Yee for excellent technical assistance. J.P. is a scholarship holder within the projects "Scholarship support for PhD students specializing in majors strategic for Wielkopolska's development", Sub-measure 8.2.2 Human Capital Operational Programme, co-financed by the EU under the European Social Fund and the Polish National Science Centre "Etiuda" for PhD students under fellowship 2013/08/T/NZ7/00241. This study was supported by the National Science Centre under grants N N401 067238 and 2012/05/N/NZ7/00624, the European Fund for Regional Development No UDA-POIG.02.01.00-30-182/09, and funds from the University of the Pacific, Arthur A. Dugoni School of Dentistry.

Keywords: antitumor agents · diazepines · liposomes · photodynamic therapy · porphyrazines

[1] S. Yano, S. Hirohara, M. Obata, Y. Hagiya, S.-I. Ogura, A. Ikeda, H. Kataoka, M. Tanaka, T. Joh, *J. Photochem. Photobiol. C* **2011**, *12*, 46 – 67.
[2] R. R. Allison, C. H. Sibata, *Photodiagn. Photodyn. Ther.* **2010**, *7*, 61 – 75.
[3] K. Konopka, T. Goslinski, *J. Dent. Res.* **2007**, *86*, 694 – 707.
[4] T. J. Dougherty, C. J. Gomer, B. W. Henderson, G. Jori, D. Kessel, M. Korbelik, J. Moan, Q. Peng, *J. Natl. Cancer Inst.* **1998**, *90*, 889 – 905.
[5] M. Ethirajan, Y. Chen, P. Joshi, R. K. Pandey, *Chem. Soc. Rev.* **2011**, *40*, 340 – 362.
[6] T. Goslinski, J. Piskorz, *J. Photochem. Photobiol. C* **2011**, *12*, 304 – 321.
[7] N. D. Hammer, S. Lee, B. J. Vesper, K. M. Elseth, B. M. Hoffman, A. G. M. Barrett, J. A. Radosevich, *J. Med. Chem.* **2005**, *48*, 8125 – 8133.
[8] A. L. Gryshuk, Y. Chen, W. Potter, T. Ohulchansky, A. Oseroff, R. K. Pandey, *J. Med. Chem.* **2006**, *49*, 1874 – 1881.
[9] T. Goslinski, T. Osmalek, K. Konopka, M. Wierzchowski, P. Fita, J. Mielcarek, *Polyhedron* **2011**, *30*, 1538 – 1546.
[10] E. R. Trivedi, A. S. Harney, M. B. Olive, I. Podgorski, K. Moin, B. F. Sloane, A. G. M. Barrett, T. J. Meade, B. M. Hoffman, *Proc. Natl. Acad. Sci. USA* **2010**, *107*, 1284 – 1288.
[11] M. P. Donzello, C. Ercolani, P. A. Stuzhin, A. Chiesi-Villa, C. Rizzoli, *Eur. J. Inorg. Chem.* **1999**, 2075 – 2084.
[12] S. Angeloni, C. Ercolani, *J. Porphyrins Phthalocyanines* **2000**, *4*, 474 – 483.
[13] M. P. Donzello, D. Dini, G. D'Arcangelo, C. Ercolani, R. Zhan, Z. Ou, P. A. Stuzhin, K. M. Kadish, *J. Am. Chem. Soc.* **2003**, *125*, 14190 – 14204.
[14] P. A. Stuzhin, P. Tarakanov, S. Shiryaeva, A. Zimenkova, O. I. Koifman, E. Viola, M. P. Donzello, C. Ercolani, *J. Porphyrins Phthalocyanines* **2012**, *16*, 968 – 976.
[15] M. P. Donzello, C. Ercolani, L. Mannina, E. Viola, A. Bubnova, O. Khelevina, P. A. Stuzhin, *Aust. J. Chem.* **2008**, *61*, 262 – 272.
[16] K. Plaetzer, B. Krammer, J. Berlanda, F. Berr, T. Kiesslich, *Lasers Med. Sci.* **2009**, *24*, 259 – 268.
[17] T. Goslinski, J. Piskorz, D. Brudnicki, A. J. P. White, M. Gdaniec, W. Szczolko, E. Tykarska, *Polyhedron* **2011**, *30*, 1004 – 1011.
[18] J. Piskorz, E. Tykarska, M. Gdaniec, T. Goslinski, J. Mielcarek, *Inorg. Chem. Commun.* **2012**, *20*, 13 – 17.
[19] E. Paszko, C. Ehrhardt, M. O. Senge, D. P. Kelleher, J. V. Reynolds, *Photodiagn. Photodyn. Ther.* **2011**, *8*, 14 – 29.
[20] Y. N. Konan, R. Gurny, E. Allémann, *J. Photochem. Photobiol. B* **2002**, *66*, 89 – 106.
[21] P. Skupin-Mrugalska, J. Piskorz, T. Goslinski, J. Mielcarek, K. Konopka, N. Düzgüneş, *Drug Discovery Today* **2013**, *18*, 776 – 784.
[22] C. S. Jin, G. Zheng, *Lasers Surg. Med.* **2011**, *43*, 734 – 748.
[23] S. L. J. Michel, B. M. Hoffman, S. M. Baum, A. G. M. Barrett, "Peripherally Functionalized Porphyrazines: Novel Metallomacrocycles with Broad, Untapped Potential" in *Progress in Inorganic Chemistry, Vol. 50* (Ed.: K. D. Karlin), Wiley, New York, **2001**, pp. 473 – 590.
[24] W. Szczolko, L. Sobotta, P. Fita, T. Koczorowski, M. Mikus, M. Gdaniec, A. Orzechowska, K. Burda, S. Sobiak, M. Wierzchowski, J. Mielcarek, E. Tykarska, T. Goslinski, *Tetrahedron Lett.* **2012**, *53*, 2040 – 2044.
[25] A. P. Castano, T. N. Demidova, M. R. Hamblin, *Photodiagn. Photodyn. Ther.* **2004**, *1*, 279 – 293.
[26] V. Chauke, M. Durmus, T. Nyokong, *J. Photochem. Photobiol. A* **2007**, *192*, 179 – 187.
[27] R. Bonnett, G. Martinez, *Tetrahedron* **2001**, *57*, 9513 – 9547.
[28] L. Sobotta, P. Fita, W. Szczolko, M. Wrotynski, M. Wierzchowski, T. Goslinski, J. Mielcarek, *J. Photochem. Photobiol. A* **2013**, *269*, 9 – 16.
[29] I. Seotsanyana-Mokhosi, N. Kuznetsova, T. Nyokong, *J. Photochem. Photobiol. A* **2001**, *140*, 215 – 222.

[30] S. Lijewski, J. Piskorz, M. Kucińska, M. Wierzchowski, K. Czerniak, H. Billert, M. Murias, J. Mielcarek, T. Goslinski, *Inorg. Chem. Commun.* **2013**, *29*, 97 – 100.
[31] W. Spiller, H. Kliesch, D. Wöhrle, S. Hackbarth, B. Röder, G. Schnurpfeil, *J. Porphyrins Phthalocyanines* **1998**, *2*, 145 – 158.
[32] J. Piskorz, P. Skupin, S. Lijewski, M. Korpusinski, M. Sciepura, K. Konopka, S. Sobiak, T. Goslinski, J. Mielcarek, *J. Fluorine Chem.* **2012**, *135*, 265 – 271.
[33] E. G. Sakellariou, A. G. Montalban, S. L. Beall, D. Henderson, H. G. Meunier, D. Phillips, K. Suhling, A. G. M. Barrett, B. M. Hoffman, *Tetrahedron* **2003**, *59*, 9083 – 9090.
[34] M. Wierzchowski, L. Sobotta, P. Skupin-Mrugalska, J. Kruk, W. Jusiak, M. Yee, K. Konopka, N. Düzgüneş, E. Tykarska, M. Gdaniec, J. Mielcarek, T. Goslinski, *J. Inorg. Biochem.* **2013**, *127*, 62 – 72.
[35] N. Düzgüneş, *Methods Enzymol.* **2003**, *367*, 23 – 27.
[36] J. T. F. Lau, P.-C. Lo, W.-P. Fong, D. K. P. Ng, *J. Med. Chem.* **2012**, *55*, 5446 – 5454.
[37] D. Kessel, Y. Luo, Y. Deng, C. K. Chang, *Photochem. Photobiol.* **1997**, *65*, 422 – 426.
[38] R. D. Almeida, B. J. Manadas, A. P. Carvalho, C. B. Duarte, *Biochim. Biophys. Acta Rev. Cancer* **2004**, *1704*, 59 – 86.
[39] M. Kryjewski, M. Nowak, P. Kasprzycki, P. Fita, C. Radzewicz, T. Goslinski, J. Mielcarek, *Inorg. Chem. Commun.* **2013**, *27*, 56 – 59.
[40] A. Ogunsipe, D. Maree, T. Nyokong, *J. Mol. Struct.* **2003**, *650*, 131 – 140.
[41] T. Goslinski, T. Osmalek, J. Mielcarek, *Polyhedron* **2009**, *28*, 3839 – 3843.
[42] M. Durmuş, V. Ahsen, T. Nyokong, *J. Photochem. Photobiol., A* **2007**, *186*, 323 – 329.
[43] K. Matsumoto, M. Horikoshi, K. Rikimaru, S. Enomoto, *J. Oral Pathol. Med.* **1989**, *18*, 498 – 501.
[44] S. S. Prime, S. V. R. Nixon, S. I. J. Crane, A. Stone, J. B. Matthews, N. J. Maitland, L. Remnant, S. K. Powell, S. M. Game, C. Scully, *J. Pathol.* **1990**, *160*, 259 – 269.
[45] R. D. Fields, M. V. Lancaster, *Am. Biotechnol. Lab.* **1993**, *11*, 48 – 50.
[46] K. Konopka, E. Pretzer, P. L. Felgner, N. Düzgüneş, *Biochim. Biophys. Acta Mol. Cell Res.* **1996**, *1312*, 186 – 196.

Received: March 25, 2014
Published online on ■■ ■■, 0000

Waiting for cell death: The photochemical properties and photodynamic activity of three porphyrazines containing annulated diazepine rings were investigated. The in vitro photodynamic activity of the porphyrazines and their liposomal formulations were examined by using two oral squamous cell carcinoma cell lines.

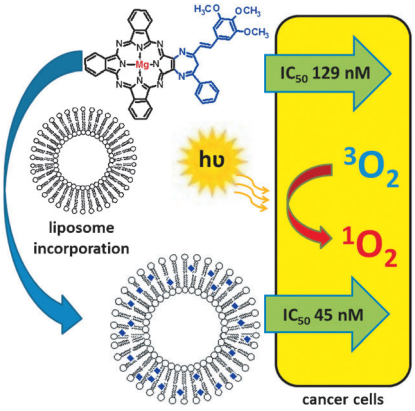

J. Piskorz, K. Konopka, N. Düzgüneş, Z. Gdaniec, J. Mielcarek, T. Goslinski**

■■ – ■■

Diazepinoporphyrazines Containing Peripheral Styryl Substituents and Their Promising Nanomolar Photodynamic Activity against Oral Cancer Cells in Liposomal Formulations